Dual Clutch Transmission Vibrations during Gear Shift: A Simulation-Based Approach for Clunking Noise Assessment

2019-01-1553

Dual Clutch Transmission Vibrations During Gear Shift: a Simulation-Based Approach for Clunking Noise Assessment

Author, co-author (Do NOT enter this information. It will be pulled from participant tab in MyTechZone)

Affiliation (Do NOT enter this information. It will be pulled from participant tab in MyTechZone)

Abstract

A novel methodology, for the assessment of Dual Clutch Transmission vibrations during gear shifts, is proposed in this paper. It is based on the capability to predict through numerical simulation a typical dynamic quantity used to objectively evaluate the vibrational behavior of a gearbox during experimental tests, i.e. the acceleration of a point on the external surface of the gearbox housing. To achieve this result, a two-step approach is proposed: an accurate simulation of the internal transmission dynamics and an offline uncoupled computation of the gearbox housing acceleration from the output of the simulation. The first step required the definition of a suitable nonlinear lumped parameter model of the car equipped with a DCT that was implemented in Amesim software. The second step, developed as a post processing tool in Matlab, is based on the knowledge of the inertance Frequency Response Functions (FRFs) between a single component of force applied in a bearing and a single component of acceleration in the measurement point. The indices used to assess the clunk severity are peak to peak amplitude and RMS of the gearbox housing acceleration. The effectiveness of this method is proven by comparing experimental and simulated trends of the clunk indices.

Introduction

In recent years, an ever-increasing number of vehicles have featured Dual Clutch Transmission technology to ensure fast gear-shifting with uninterrupted torque transfer to the driving wheels, and thus achieving high performance in terms of sportiness as well as efficiency.

Research and Development (R&D) departments are constantly engaged to improve the NVH performance of this technology. In [1] Qatu et al. present an overview of automotive NVH issues, describing the interior noise due to different sources, as powertrain, road-tyre interface and wind. As far as driveline NVH is concerned, gear whine, clutch shudder and clunking noises are analysed, giving details about their frequency ranges and their possible cause.

A potential NVH issue, that is typical of transmission systems sharing the same components of a manual transmission (MT), is the clunk noise generation during gear shift. It is directly perceivable in the car cabin as a metallic impact noise, which therefore must be carefully taken into account starting from the early design stage of the transmission. More specifically, highly efficient mechanical architectures typical of AMT and Dry-DCT layouts, while providing better fuel economy are more prone to NVH concerns due to their low level of damping and power losses.

Hence, it is becoming increasingly more important to integrate in the design process a reliable simulation methodology, able to predict the gearshift-induced vibrations, for carefully comparing different design solutions. The first step in this direction is the development of a detailed transmission model able to describe the internal dynamics of the gearbox and to highlight the NVH phenomenon of interest. More specifically, the clunking noise, which is due to backlash traversal, is mentioned in [2], where Gear Shift Patterns are optimized to satisfy different customers' requirements, like drivability, NVH performance, emissions and fuel consumption. At least total transmission backlash, driveshaft stiffness and gears inertia should be taken into account to model this type of vibration. In [3], a DCT model is developed to investigate the low frequency clunk. From an experimental point of view in [4] six powertrain noise and vibration troubleshooting case studies are presented to prove techniques and engineering tools to address a variety of drivetrain NVH issues. Another typical gearbox vibration is the gear rattle, which is an impact-induced noise caused by unloaded gear pairs excited by the engine orders. It has been treated by Brancati et al., discussing the squeeze effect of the oil between the teeth with a theoretical model in [5]. From further examination of the experimental results, varying the lubrication mechanism, positive influence of oil damping factor in reducing the impacts and thus rattle vibrations was demonstrated [6]. Modifications on the clutch stiffness parameter have strong influence on the gear rattle intensity [7], which is not caused by a vibration mode excitation of the driveline. The hysteresis seems to have an optimum range of values, resulting in vibration level increment when it is over dimensioned. Other possible investigation processes are conducted using wavelet analysis [8] for gear rattle analysis in transmission unloaded gears, or deviation of peak force from the average value [9] to assess rattle severity.

In [10] the authors proposed a methodology for the assessment of the NVH performance of (DCTs) depending on some transmission design parameters, e.g. torsional backlash in the synchronizers or clutch disc moment of inertia, during low speed maneuvers, evaluating benefits in terms of RMS value of each bearing force time-history.

In [11] the potentiality of reducing noise and vibration of a vehicle transmission thanks to powertrain control integration with active braking is investigated. The idea is to apply a torsional preload to the transmission system so that the immunity to external disturbances coming from the road of from the input shaft significantly increases.

The proposed nonlinear lumped parameters model is extremely accurate in the description of the synchronizer dynamics, which include a customized modelling of the contact between the plunger ball and synchronizer sleeve groove. In [12] the response of a DCT, during gear synchronization is analyzed using a powertrain model with lumped inertias. Simulations proved the highly nonlinear nature of synchronizer and through the introduction of harmonic engine torques, increased vibration of the synchronizer sleeve results, with excitations in the engaging mechanism. Sleeve and synchronizer blocker ring pointing angle (roof angle) must be designed to maintain index torque above the drag torque in every gear position to preserve gear engagement. Although shift quality is not directly affected by the synchronizers, smooth and quick transition of gears is logically a significant factor in accomplishing the fuel economy objective [13].

The proposed methodology can be effectively used to analyze and investigate from the NVH perspective, the effect of different transmission layout (e.g. geometrical disposition of the transmission shafts and meshing gears in the space), bearings location, gearbox housing design, gears macro-geometry parameters, backlashes, rotating parts inertia and drag torques.

This paper begins with a general description of the analyzed DCT mechanical architecture. Then the two-step methodology, with the description of the model and the gearbox acceleration evaluation tool is proposed. The gear shift manoeuver used for the experimental validation of the model is then described. Finally, results and benefits from the application of the proposed methodology are presented comparing the clunking noise assessment with the improvements revealed during experimental tests.

The Dual Clutch Transmission: layout and mechanical architecture

The main characteristic of a DCT is the presence of two clutches, fully integrated in a dual clutch unit (DCU), which may be of dry or wet-type, according to the amount of torque that must be transferred through them. In the considered Dry-DCT case, the driven disk of each clutch (K1 and K2) is mounted on one of the two coaxial primary shafts, PS1 carrying the odd gears and PS2 the even ones. The control unit manages gearshifts and engagements/disengagements of clutches. The advantage of a DCT gearbox is the possibility of transferring torque without traction interruption, due to the controlled slippage of the clutches. The two clutches are alternatively engaged for even and odd gears. The disengagement of the off-going clutch and the engagement of the on-coming one is managed by an electronically controlled shift process. During the start-up phase, the two clutches are disengaged, the first gear is engaged therefore no torque is transferred from engine to the wheels. When the odd clutch K1 starts engaging an increasing torque is transferred from the inner primary shaft PS1 to the secondary shaft through the first gear pair. Meanwhile, it is possible to preselect the second gear if not already engaged, being the second even clutch K2 disengaged. This concept allows to understand the potential of a DCT gearbox. Indeed, it is possible to engage the corresponding synchronizer in advance with respect to the effective actuation of the next gear that is achieved engaging the associated clutch. The clutch to clutch shift procedure together with the preselection of the new gear eliminate the dead times due to the traditional synchronization phase of an AMT. Moreover, the DCT compensates and overcomes the dynamic limits of an Automated Manual Transmission (AMT), reaching better dynamic performance during vehicle acceleration and more comfortable driving thanks to continuous torque transmission during the gearshifts. In contrast to AMT, a distinctive characteristic of DCT is that the synchronizers are mounted between two non-consecutive gears thus enabling, in case of a sequential gear-shift, the preselection of the next gear without removing the actual one (view Figure 1). Moreover, the Electronic Control Unit (TCU) avoids the simultaneous lock of the two clutches thus preventing structural damages to the gearbox.

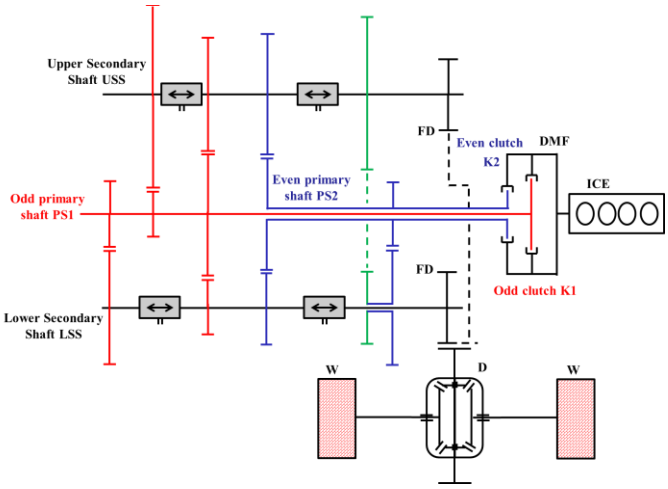

Figure 1. Layout of a DCT.

Note that in the schematic view of Figure 1, the axes of the two primary shafts, the two secondary shafts and the differential do not belong to the same plane, but they are arranged in the space to form a compact solution.

Two step methodology for gearshift vibration assessment

In this section the proposed methodology for gearshift vibrations assessment of a DCT is explained in detail. It consists in a two-step approach with firstly an accurate simulation of the internal transmission dynamics and subsequently an offline uncoupled computation of the gearbox housing acceleration from the output of the simulation.

1st step: Amesim model

A nonlinear lumped parameter model has been developed in Amesim environment to study the inner dynamics of a DCT gearbox and the longitudinal vehicle dynamics of a mid-size sedan. The nonlinear behavior of the transmission is mainly due to the presence of backlash between the teeth of gears engaged on primary and

secondary shafts, on the differential and in the internal elements of the synchronizer. The main model features and assumptions are:

- the model can be set to simulate manoeuvers with one or two synchronizers engaged at the same time and, with an accurate level of details for the synchronization phase;
- the torsion of the transmission shafts is taken into account introducing rotation stiffness and damping characteristics: primary and secondary shafts are modelled as a series of inertia ad stiffness elements;
- the inputs of the model are the gear shift forks displacement, the engine torque and the clutches transmissible torques;
- the effects of temperature variations are not considered and load dependence of bearing losses is neglected.

A global overview of the Amesim model is proposed in Figure 2, where the main subsystems are identified. The engine torque time history is applied to the primary mass of a Dual Mass Flywheel (bottom right), while the secondary mass is connected to the clutch drum of the DCU. The clutches transmissible torque signals enter into friction model blocks that computes the actual clutch torques transferred through them. The gear shift forks positions are the inputs that control the gear synchronization, engagement and disengagement according to the specific maneuver that must be tested. The vehicle model is a one DOF pure longitudinal model, while each tire is modelled thorough a transient formulation of Pacejka's magic formulas.

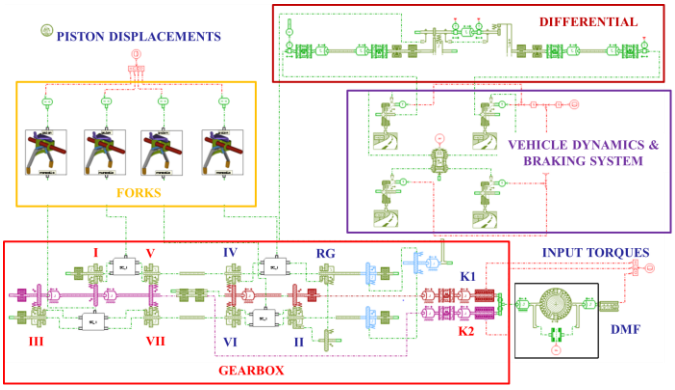

Figure 2. Amesim model layout.

Transmission layout

The engine torque time history is applied to the first inertia of the system that includes the engine and the first mass of the DMF, while its second mass together with inertia of the clutches mechanism are accounted in the second inertia after DMF. The DMF model takes into account the variation of the elastic and damping characteristics with the rotational speed. For both clutches, a lumped torsional stiffness and damping in parallel and an angular clearance are implemented to model the splined connection between the driven clutch hub and the primary shaft. The transmission includes seven gears, the driving gears (pinions) are fixed to the primary shaft, while the driven idle gears (wheels) are mounted on the secondary shafts. The primary shafts are modelled as a series of lumped inertia elements, including both the inertia of driving gears and shaft, and torsional stiffness elements, while for the secondary shafts the inertia of shaft is coupled with the inertia of the synchronizers. Moreover, the driven gears model includes inertia, contact stiffness and damping, clearance of the gear meshing and geometry parameters like pitch radius, pressure and helix angles, and Young modulus. The forks model receives as input the piston displacements of the hydraulic actuator and generates a force command to the sleeve of each synchronizer. The clearance between the shift finger and the fork gate and the bending stiffness of the fork arms are taken into account. A flexible shaft with viscous damping is assumed to model the two half-shafts. Absolute bearings models (i.e. with the external ring still) are mounted on primary and secondary shafts and on differential shaft considering a constant torque loss. Relative bearings are inserted between primary and secondary shafts and seal models are added the output shafts of the differential. Finally, a basic vehicle model, considering only the longitudinal dynamics is coupled with a nonlinear Pacejka tyre model [14] and a simple braking system with different parameters for front and rear brakes.

Synchronizer model

The synchronizer model takes into account both the torsional and the axial behavior of its inner elements. It is modelled in order to describe, with a high level of detail, the dynamics during the synchronization phase and gear engagement, starting from the central position of the sleeve to the complete engagement of sleeve dog teeth with idle gear dog teeth. In Figure 3 the detailed synchronizer model is reported, putting in evidence the separation between axial and torsional behaviour.

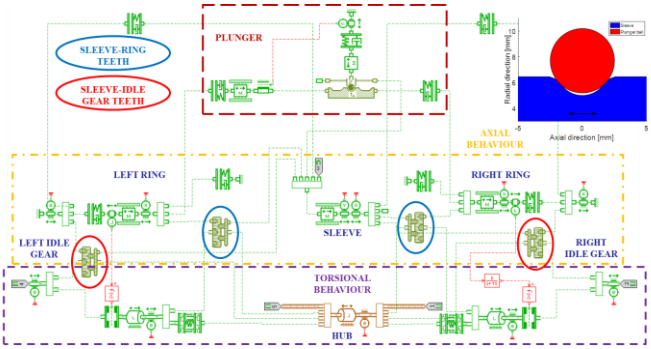

Figure 3. Synchronizer Amesim model.

This model considers 9 DOFs that can be summarized as:

- axial displacement of the sleeve;
- radial and axial displacements of the plunger ball;
- axial and rotational displacements of left and right rings;
- rotation of the two idle gears on the two side of the synchronizer.

As for the plunger, the preloaded ball moves in the axial direction towards the gear to be engaged; the plunger is dragged through the internal groove of the sleeve. The choice to use a cam profile contact (as illustrated in the top right of Figure 3) to model the plunger/sleeve interaction ensures higher accuracy, if compared with a more standard nonlinear axial stiffness and damping model. Moreover, an axial clearance with relative end-stop condition is considered between the plunger and the two rings of the synchronizer. Axial clearances are placed between ring and hub, and between ring and idle gear. A torsional clearance is modelled between the hub and the two blocker rings, while no torsional backlash has been modelled between hub and sleeve since it is usually very small. Finally, the dog teeth profiles have been defined for sleeve, rings and idle gears.

Bearing force computation

The bearing force computation is implemented in Amesim model with a customized procedure that, starting from the radial, tangential and axial forces exchanged by the gears of primary and secondary shafts, is able to evaluate the force on each bearing of the transmission in the axial and radial direction. In Figure 4 it is possible to appreciate the relative position of the gearbox shafts and the reference frames (local and global) introduced for the bearing force computation. The global reference system, depicted with black arrows in the figure, is characterized by the axial direction (X), i.e. parallel to the axis of the transmission shafts, and two perpendicular radial directions (Y and Z).

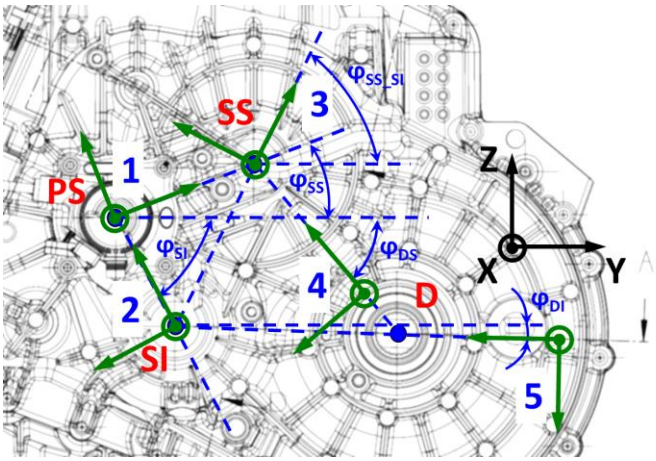

Figure 4. Local and global reference system.

Five local reference frames are introduced (green arrows) to be used for the computation of the forces exchanged between each pair of meshing gears. They refer to the interaction between:

1. Primary Shaft (PS) and upper secondary shaft (SS);
2. Primary Shaft (PS) and lower secondary shaft (SI);
3. Upper secondary shaft (SS) and lower secondary shaft (SI);
4. Upper secondary shaft (SS) and Differential (D);
5. Lower secondary shaft (SI) and Differential (D).

The radial direction of these local reference systems corresponds to the line connecting the center of the shafts involved, the axial direction is parallel to the shafts axis and the tangential direction is tangent to the pitch circumferences and with a sense consistent with a right-handed coordinate system. The forces exchanged by the gears during the simulation are evaluated starting from the torque exchanged by each couple of driving and driven gears, mounted respectively on primary and secondary shaft. The three components of the meshing force, i.e. tangential, radial and axial, are calculated using Eq. 1:

$$\begin{cases} T = \frac{Torque}{r_p} \\ R = T\frac{\tan\alpha}{\cos\beta} \\ A = T\tan\beta \end{cases} \quad (1)$$

where r_p is the pitch radius, α is the pressure angle, and β is the helix angle of the gear involved. The following step consists in evaluating the radial component of the reaction force on each bearing. The two primary shafts are considered as a single shaft in which all the driving gears are mounted, while bearings and gearbox case are considered infinitely stiff. The bending of gearbox shafts is neglected, and thus only torsional dynamics are taken into account. The process to evaluate the bearing forces takes into account shaft disposition in the gearbox, therefore it is necessary to calculate the reaction forces on the bearings for each couple of shaft and then apply the superposition principle after converting these forces in the global reference system. Radial forces of the bearings are evaluated in the local reference system writing moment equilibrium equations for each transmission shaft, as it is done for the upper secondary shaft (SS) using the Eq. 2:

$$\begin{cases} \sum_{i=1}^{N}\left(A_{SS_i}r_{p_i} + R_{SS_i}d_i\right) + F_{R_B}l = 0 \\ \sum_{i=1}^{N}\left(R_{SS_i}\right) + F_{R_A} + F_{R_B} = 0 \\ \sum_{i=1}^{N}\left(T_{SS_i}d_i\right) + F_{T_B}l = 0 \\ \sum_{i=1}^{N}\left(T_{SS_i}\right) + F_{T_A} + F_{T_B} = 0 \end{cases} \quad (2)$$

where r_{p_i} and d_i are respectively the pitch radius and the distance from the bearing on the left (A) of all the gears that are on the SS shaft, while T_{SS_i}, R_{SS_i}, and A_{SS_i} are the forces on the gear of the SS shaft and F_{R_A}, F_{R_B}, F_{T_A}, F_{T_B} are the reaction force of the bearing A and B in radial and tangential direction.

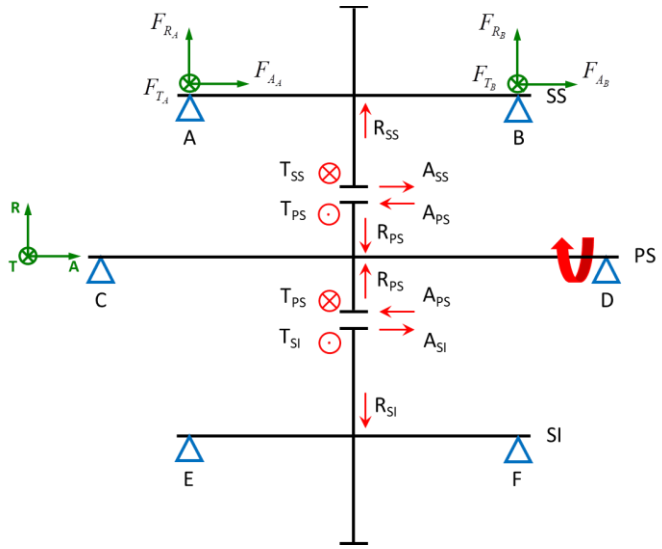

Figure 5. Forces on primary and secondary shafts.

For the differential, in addition to the forces between pinions and crown it is necessary to evaluate the axial forces inside the differential due to the bevel gears according to Eq. 3:

$$\begin{cases} T_{hs} = \frac{|Torque_{hs}|}{r_{p_{hs}}} \\ A_{hs} = 2T_{hs}\tan\alpha_c\cos\gamma \end{cases} \quad (3)$$

where $r_{p_{hs}}$ is the pitch radius, α_c is the pressure angle, γ is the semi-pitch cone angle of the bevel gear, while $Torque_{hs}$ is the torque of each half-shaft of the car. After having computed the total axial load applied on each shaft due to helical gears, the axial force distribution among the two tapered roller bearings is evaluated in accordance with the equations reported in SKF manual [15] for an X mounting arrangement.

2nd step: Gearbox housing acceleration computation

The second step of the proposed methodology starts from the output quantities of the Amesim model, namely the components of the bearing reaction forces, which are imported in Matlab for a post-processing algorithm.

Application of superposition principle

The approach is based on the knowledge of the FEM model inertances FRFs between the single component of force (X, Y, Z direction in a global reference frame) applied in a bearing and a single component of acceleration (X,Y,Z direction) in the measurement point. By combining the FRFs and the time-histories of the previously calculated forces, the multiple-input single-output (MISO) response of the dynamic system supposed linear is evaluated, through the application of the superposition principle, as it is possible to appreciate from Eq. 4, where the elements of the matrix are the frequency response functions:

$$\begin{Bmatrix} a_X \\ a_Y \\ a_Z \end{Bmatrix} = \begin{bmatrix} a_X/F_{X_A} & \cdots & a_X/F_{X_H} & a_X/F_{Y_A} & \cdots & a_X/F_{Y_H} & a_X/F_{Z_A} & \cdots & a_X/F_{Z_H} \\ a_Y/F_{X_A} & \cdots & a_Y/F_{X_H} & a_Y/F_{Y_A} & \cdots & a_Y/F_{Y_H} & a_Y/F_{Z_A} & \cdots & a_Y/F_{Z_H} \\ a_Z/F_{X_A} & \cdots & a_Z/F_{X_H} & a_Z/F_{Y_A} & \cdots & a_Z/F_{Y_H} & a_Z/F_{Z_A} & \cdots & a_Z/F_{Z_H} \end{bmatrix} \begin{Bmatrix} F_{X_A} \\ \vdots \\ F_{X_H} \\ F_{Y_A} \\ \vdots \\ F_{Y_H} \\ F_{Z_A} \\ \vdots \\ F_{Z_H} \end{Bmatrix} \quad (4)$$

The inertances computation from the dynamic Finite Element Model of the assembled powertrain, which includes engine and transmission, is based on the assumption of free-free boundary conditions. It results a good approximation, in the mid to high frequency range, considering that the engine mounts create a very soft connection between the powertrain and the vehicle frame. In Figure 6 the measurement point P of the gearbox housing acceleration, used for the chunking noise assessment, is highlighted; moreover also the front and rear bearings positions are indicated for each shaft.

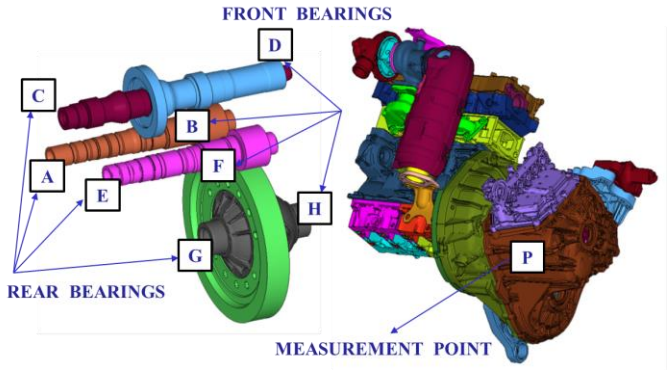

Figure 6. Bearings and measurement point.

The use of a FEM model lead to consider the gearbox housing as a MDOF linear system. Moreover, the nonlinear torsional dynamics of the transmission and the gearbox housing vibration are supposed completely uncoupled, hence the proposed approach allows to compute the acceleration of the gearbox points as a post processing tool with respect to the Amesim model simulation. The torsional dynamics of the DCT is considered as the only source of the forces applied to the gearbox.

Gearbox housing FRF

The directions of the global reference system, reported in black in Figure 4, correspond to the same directions of the CAD model reference system. In Figure 7, the FEM inertances evaluated in the X direction, by applying an impulse in X, are reported. They give an information on the axial dynamic and it is possible to appreciate that the gearbox vibration due to a force applied at the two bearings in the lower secondary shaft (E and F) is predominant for frequencies below 1500 Hz, while at higher frequencies bearings on the differential (G and H) have a remarkable participation factor.

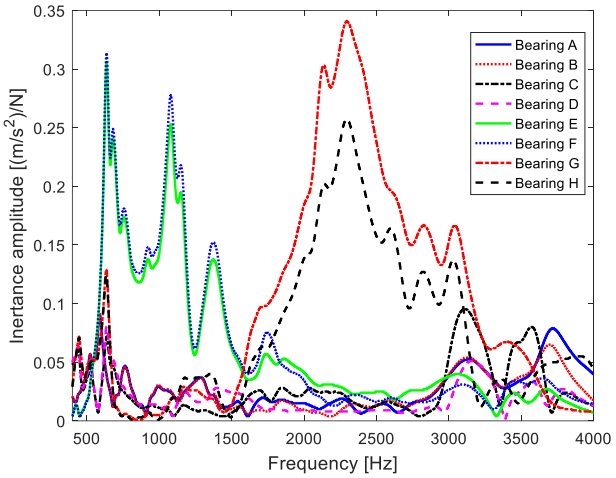

Figure 7. Inertances from bearings forces in X direction and gearbox acceleration in X direction.

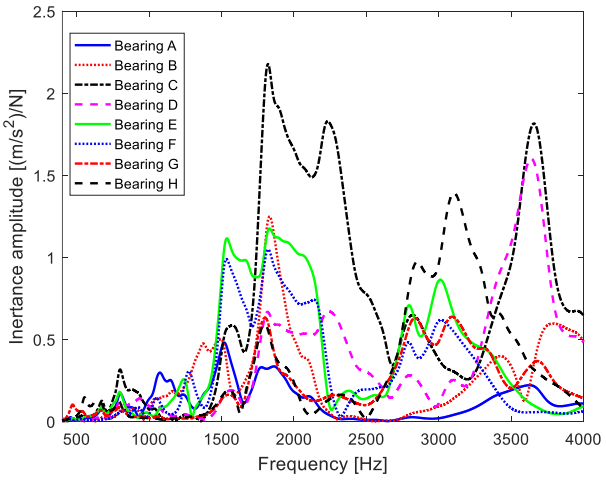

Figure 8. Inertances from bearings forces in Y direction and gearbox acceleration in Y direction.

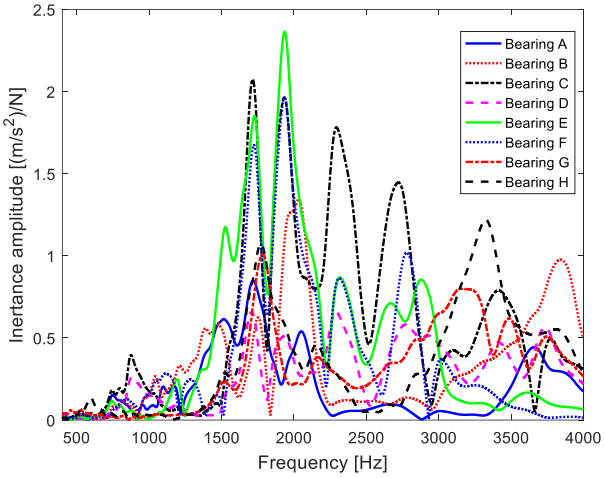

Figure 9. Inertances from bearings forces in Z direction and gearbox acceleration in Z direction.

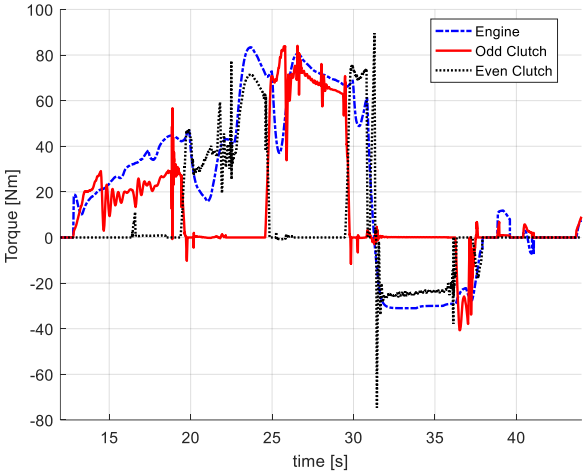

Figure 10. Torques of engine and clutches.

In Figure 8 and Figure 9 the bearings FRFs in Y and Z directions, considering an impulse respectively in Y and Z direction in the measurement point, are reported. The FRFs trends shows high peaks in the frequency range above 1500 Hz.

Algorithm

Starting from the assumption that the FEM model of the assembled powertrain is linear, the response of such system can be computed by performing the time-domain convolution of the excitation (reaction forces on bearings) and the system impulse response (from FEM inertance FRFs). The impulse acceleration response is evaluated using the Inverse Fast Fourier Transform (IFFT) of the system inertance FRFs, as reported in Eq. 5:

$$\ddot{h}(t) = IFFT\left(H_{jk}(\omega)\right) = \frac{1}{2\pi}\int_{-\infty}^{\infty} H_{jk}(\omega)e^{i\omega t}\, d\omega \qquad (5)$$

where $H_{jk}(\omega)$ is the frequency response and ω the angular frequency. Once the impulse response is computed, the acceleration can be calculated by performing its convolution with the force exciting the system $u(t)$ as indicated in Eq. 6:

$$\ddot{x}(t) = \left(\ddot{h} * u\right)(t) = \int_0^{\infty} \ddot{h}(\tau)u(t-\tau)d\tau \qquad (6)$$

Gearshift manoeuvers

The validation of the Amesim model has been done comparing the simulation results with the experimental runs, that consist in a series of gearshifts in up-shift (from 1st to 4th gear) and in down-shift (from 4th to 1st) for different levels of brake pressure and with a GPP (Gas Pedal Position) of 20% with respect to the full throttle.

The input parameters of the model are the transmissible torques of the two clutches, the engine torque, the master cylinder pressure of the braking system and the piston displacements of the gearshift hydraulic actuators. In Figure 10 the input torque of the engine is reported together with the torques evaluated by the Amesim model and transmitted by the odd and the even clutches.

Actually, a DCT gearbox is controlled in closed-loop by the transmission control unit (TCU), while in the Amesim model the inputs are applied in open-loop due to the lack of the control logic. Therefore, the input signals to the transmission is not correlated to the actual working status of the system. The input torques and actuators positions time histories were collected during dedicated experimental test when the TCU variables were stored.

A constant time delay of $\tau = 0.2s$ is applied to the engine torque, while the clutches transmissible torques is increased of 2Nm to correctly tune the kiss point. Moreover, to take into account the engine idle condition, the torque of the engine is set to zero when both clutches are disengaged in order to avoid that engine stop due to engine friction.

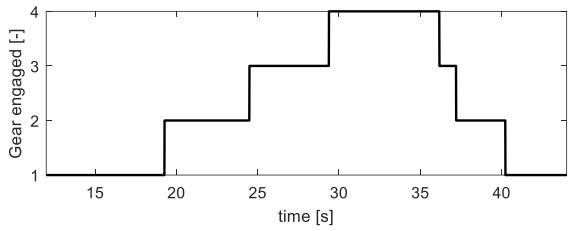

Figure 11. Time history of the actual gear engaged.

As it is possible to appreciate from Figure 10 and Figure 11 the simulation starts with the first gear engaged and both clutches open, and then it consists in a series of upshifts and downshifts. During the cross-shift phase two synchronizers are engaged: the former for the outgoing gear and the latter for the oncoming gear.

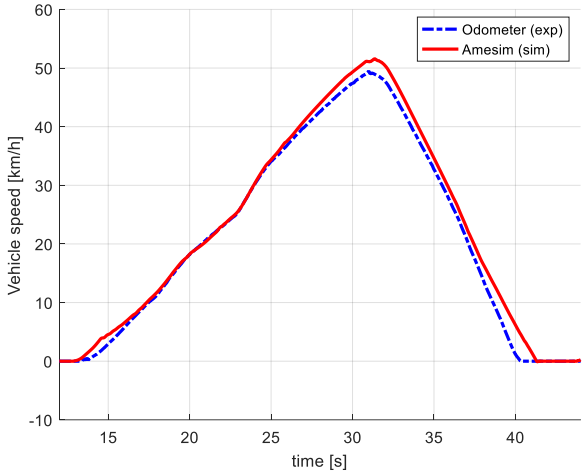

Figure 12. Vehicle speed.

The first step for the further experimental model validation consists in the load correlation w.r.t. the nominal steady-state resistance parameters, necessary to match the low frequency content of the experimental trends. This tuning process has been implemented in terms of an additional road slope applied to the Amesim model to converge to the experimental results. Another possibility could have been a change of the rolling resistance parameters or the aerodynamic coefficients, but it has been preferred to change the slope to have a bidirectional constant effect (positive and negative slope depending on the necessity). The other preliminary issue was the estimation of the gain between the master cylinder pressure, available from CAN data, and the total torque applied to the wheels, due to the lack of knowledge of the exact parameters of the vehicle braking system installed on the tested car. In Figure 12 it is possible to appreciate that the trends of the experimental and simulated vehicle speeds are very close each other after all the tuning processes.

Simulation results

Typical simulation variables for analyzing the gearshift phase are the time histories of the synchronizer sleeve axial position, and displacements of ring and plunger, as reported in Figure 13, and the angular speed of secondary shaft, synchronizer ring and idle gear during the synchronization phase, as in Figure 14. The Figure 13 represents the detail of the 2nd gear engagement and it is possible to notice the five synchronization phases, which start from the first vertical red dash-dot line and are separated by the other two lines:

- the pre-synchronization phase when the sleeve moves the plunger against the ring, the ring rotates under the action of the friction torque between the friction cones and start to lock the axial movement of the sleeve;
- the synchronization phase when the friction torque in the conic clutch is used to synchronize the rotational speed of the hub and idle gear;
- the free flying, during which the sleeve can continue its travel towards the idle gear, it passes through the ring, which no more opposes resistance, and goes until it hits the gear dog teeth of the idle gear: during this phase the sleeve can have an important linear velocity and its rotary velocity possibly does not match anymore the gear one (synchronization loss); that can result in an important shock, which is often referred to as “double bump”;
- the gear deviation phase in which after that the contact with the gear is established, the tangential force exchanged generates an aligning torque that allow deviation of the gear so that once again the sleeve path is free from obstacles;
- the lock-up phase when the sleeve dogs finish their run passing through the gear ones: thus, coupling is obtained and it is maintained thanks to back angle on dogs.

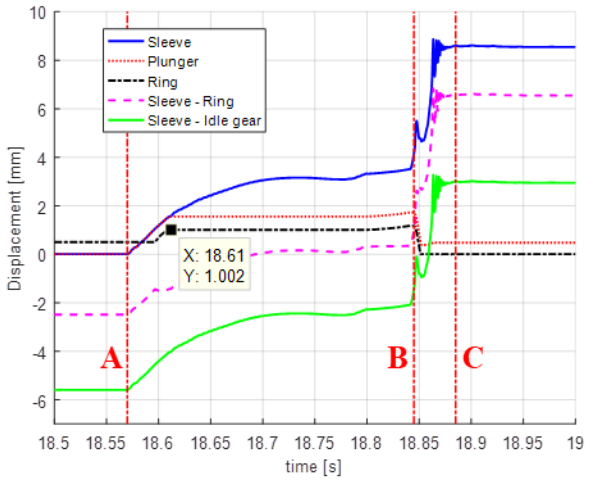

Figure 13. Axial positions of synchronizer elements.

In the first part of the time history the sleeve and the plunger ball move together, until the plunger enters in contact with the blocker ring. The synchronizer ring has a sudden acceleration, generated by the synchronization torque, and stops when it reaches the end-stop position on the hub. After a while, the idle gear angular speed starts to decrease as per effect of the friction torque between the cones and progressively reaches the synchronizer hub speed.

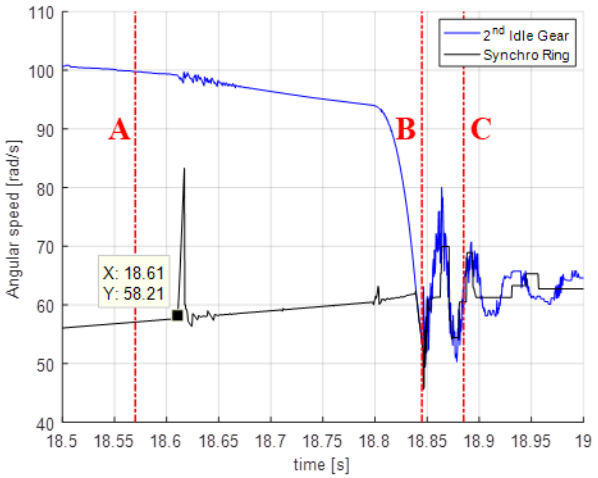

Figure 14. Angular speeds during synchronization phase.

The outputs of the Amesim model correspond to the tangential, radial and axial forces on the bearing of the transmission. In Figure 15 it is possible to appreciate the high-frequency content in the radial forces of the bearings mounted on the two secondary shafts, especially

during the gearshift phase that includes synchronization and clutch engaging phases. Moreover, the intersection between the dotted red line and the dotted blue line corresponds to the time in which the cross-shift of the two clutches happens. In fact, the forces generated by the transmission driveline are firstly absorbed by the bearings mounted on the upper secondary shaft (where the first driven gear is mounted) and then by the bearings on the lower secondary shaft (where the second driven gear is fitted).

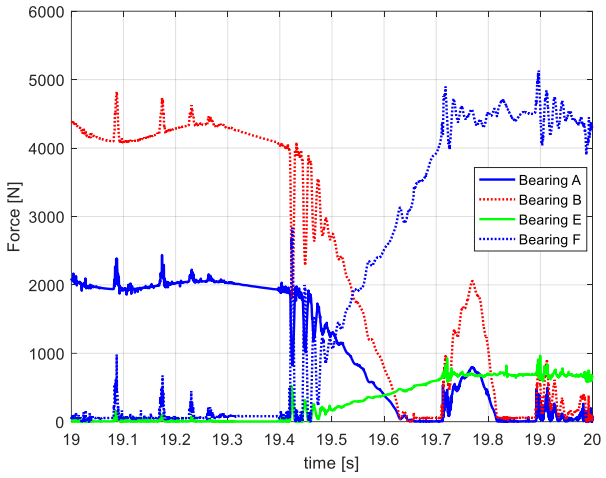

Figure 15. Radial forces on two secondary shafts bearings.

Experimental data analysis: Gearshift events producing the main acceleration peaks

Clunking noise can be recognized by analyzing the acceleration time history during the gearshift manoeuver. In fact, the acceleration measured in a point of the gearbox external surface contains information on the main events occurring during gearshift.

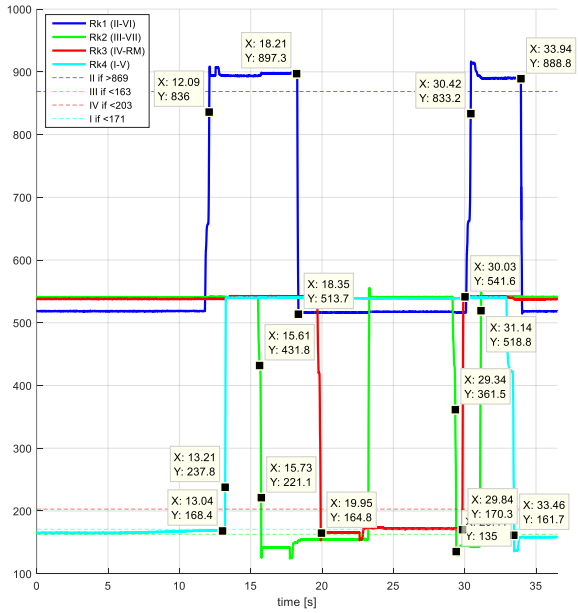

Figure 16. Gear positions.

There are five different events that produce potential NVH issues and can be related to the following phases:

- gear engagement;
- gear disengagement;
- oncoming clutch start of engagement during cross-shift;
- outgoing clutch end of engagement during cross-shift;
- zero-crossing of torque on an active (engaged) transmission path (kiss/touch point).

The first two noise sources can be clearly identified by checking the gear positions time history, reported in Figure 16, together with the accelerometer signal in Figure 17, in which the labels identify the peaks associated uniquely with the gear engagement and disengagement.

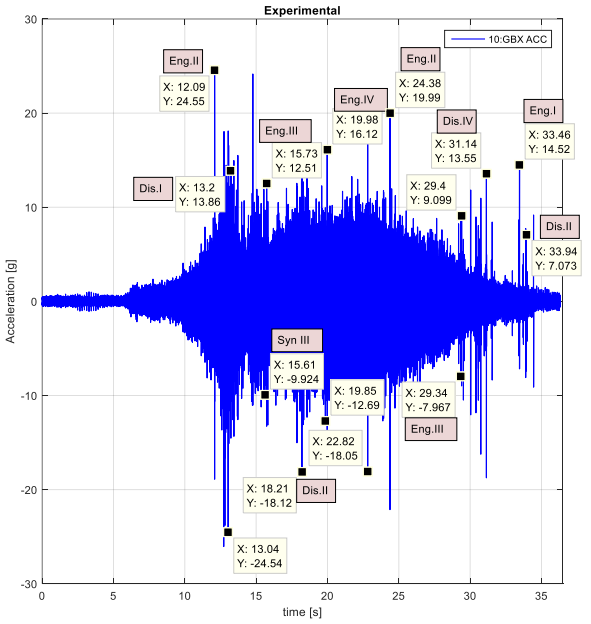

Figure 17. Gearbox housing acceleration.

The remaining main peaks in the acceleration signal are due to impacts between gear teeth due to gears backlash traversal, as it happens when the transmitted force changes its sign passing from negative to positive or inversely.

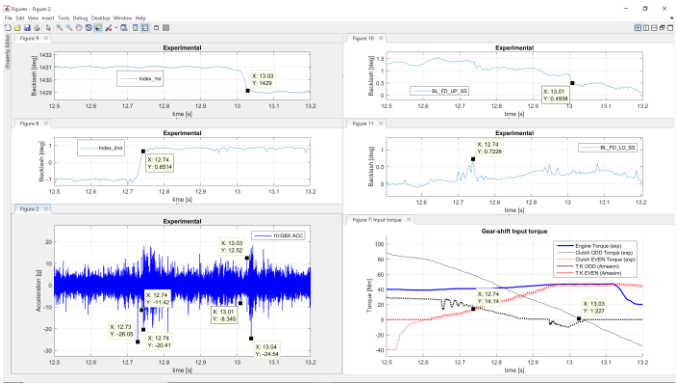

Figure 18. Cross-shift from 1st to 2nd.

From the analysis of Figure 18, where a cross-shift from first to second gear is reported, two main events can be noted during the cross-shift phase:

- start of loading on the oncoming transmission path (even gear clutch and primary shaft);
- end of loading on the offgoing transmission path (odd gear clutch and primary shaft).

A step change in variables index 2nd (a measure of the backlash in the 2nd gear synchronizer) and index 1st (a measure of the backlash in the 1st gear synchronizer) clearly show the instants of time when the impacts are generated.

Simulation results analysis

The peaks of acceleration reported in Figure 19 are clearly distinguishable and correlated to the torsional events happening in the gearbox during the gearshifts. Conversely, in the experimental acceleration signal of Figure 17 many sources of noise are inevitably present (e.g. from the road, the internal combustion engine, etc.).

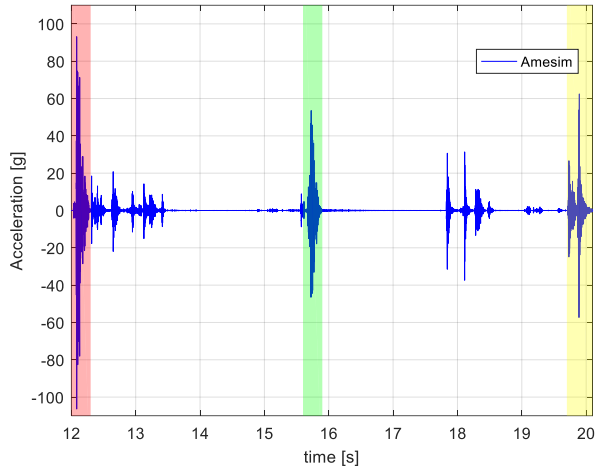

Figure 19. Simulated acceleration of the gearbox.

The comparison between model and experiment in terms of gearbox acceleration is qualitative only. Many uncertainties, as the FRF of the gearbox case or the rigid hypothesis for the shafts, the open loop input application and other unmodeled dynamics, lead inevitably to quantitative differences in the simulation results. Nevertheless, this approach can be considered valid for comparative analysis and for evaluating different design solution in terms of gearshift noise. From Figure 20 it is possible to appreciate the time history of engine, primary and secondary shafts angular speeds. The secondary speed velocity is scaled, using the gear ratio, in order to better recognize the engaging phase, corresponding to the colored area in the two figures, which are the critical phases for NVH issues.

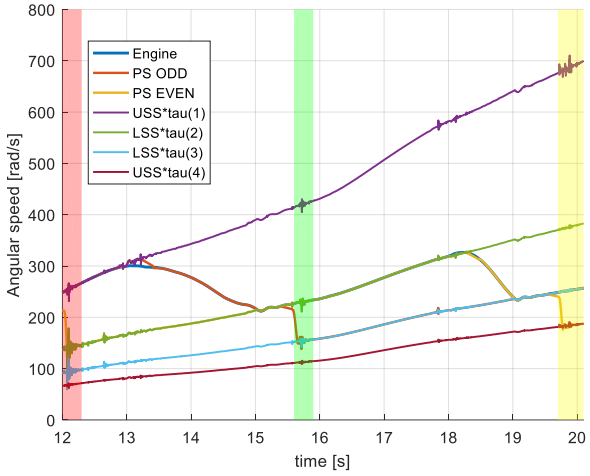

Figure 20. Simulated speeds of primary and secondary shafts.

The proposed approach could be used to analyze and estimate possible improvements in the transmission, acting on backlashes, disposition of the transmission shafts, geometry parameters of the gears and rotating part inertia. In the following section results of the sensitivity analysis, changing the inertia of different driven gear will be presented.

Case study: effects of gears inertia

Simulated NVH trends

The effects of reducing or increasing the driven gears inertia on the NVH performance is evaluated using the proposed methodology applied to the experimental manoeuver previously described. The indices used to assess the clunk severity are peak to peak amplitude and RMS of the gearbox housing acceleration. For the peak to peak comparison, only the highest peaks, inner to the colored gear engaging phases of Figure 19, are considered. The simulation results regarding the inertia effects modification are summarized in Figure 21. In it is possible to note that inertia reduction of the 2nd gear of both 7% and 3.5% worsen the 1st to 2nd gearshift but improve the 2nd to 3rd and the 3rd to 4th gearshifts. On the contrary, an increase of inertia of 3.5% improve the 2nd and 4th gear engagement and worsen the 3rd one. An excessive inertia increase up to 7% leads to a worsening of the 3rd gear engagement although a little worsening in the 1st to 2nd gearshift and an improvement in the 4th gear engagement occur. The first gearshift is the more critical for the clunking noise and therefore the inertia modifications are aimed at improving that specific gearshift. During the 4th gear engagement the NP condition is the worst, although the peak are smaller respect to the others gear engagements.

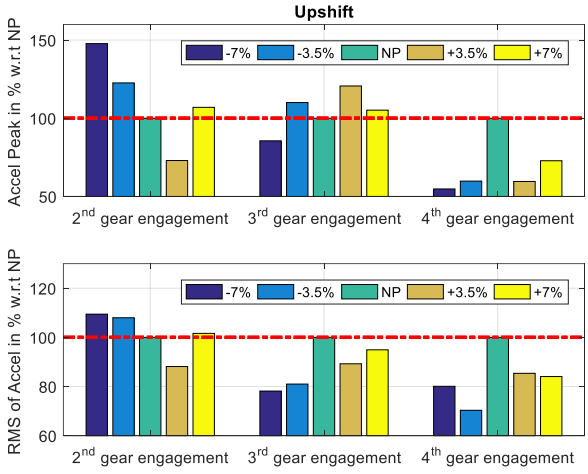

Figure 21. Upshift 2nd idle gear inertia modification.

A lower inertia of the 2nd idle gear increases its mobility, and so its tendency to accelerate. The focus is at the end of the 2nd gear engagement phase, after speed synchronization, when the dog-teeth of the synchronizer sleeve impact the dog teeth of the lightened idle gear. Higher rotational acceleration leads to higher velocity impacts and therefore higher gearbox housing acceleration peaks. It is also important to analyze the effect of the inertia reduction of the preselected 2nd idle gear during engagement of 3rd gear on the same secondary shaft. The 3rd gear engagement provokes a series of shocks which propagates through the 3rd gear synchronizer to the lower secondary shaft. The latter accelerate/decelerate and other shocks are generated in the preselected 2nd gear synchronizer, thus propagating the vibrations to the even primary shaft. The higher the inertia of the idle gear the higher the risk of NVH issues because the resistance applied during impact, i.e. the inertia torque, becomes higher.

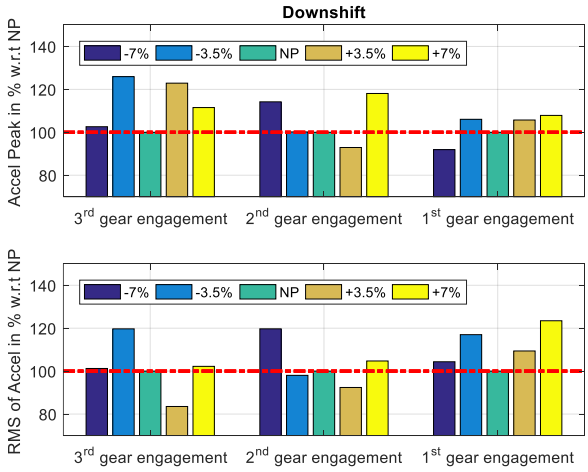

Figure 22. Downshift 2nd idle gear inertia modification.

The analysis is also extended to the downshift manoeuvers and the results are shown Figure 22. Upshift and downshift results are consistent. The trend of the peak analysis of 2nd gear engagement is very similar between the upshift and downshift manoeuvers, with a worsening for inertia reduction and an improvement for an inertia increase of 3.5%. As for the 3rd gear engagement, the NP configuration is the optimal one in both maneuvers, with a very light worsening for ±3.5% inertia modification.

As far as the gear disengagement is concerned, the axial displacement of the sleeve is less hindered when moving from sure engaged position to the neutral one if the inertia is lower. The dynamics of the unloaded primary shaft is driven by the drag torques and tends to decelerate in this phase, so a preload in the contact between the teeth is applied. Then, when the torque is re-applied to the incoming primary shaft during cross-shift, a lower idle gear inertia implies lower energy impacts between the teeth flanks (of the driving and driven gear).

Experimental validation of NVH trends

In this section, a comparison between experimental and simulated results is prosed, after a 2nd gear inertia reduction of 7%. As it is possible to appreciate from Figure 23, four acceleration peaks are analyzed, comparing the acceleration amplitude in the two case of normal production and inertia reduction. All the acceleration peaks are related to an inner event of the gearbox. In fact, as regards the two peaks, inside the colored area of acceleration time history, they are due to the synchronization impacts during 1st to 2nd upshift and during the 3rd gear engagement, as it is possible to note from the time history of forks piston displacements. The other two peaks are instead related to the cross-shift phase, during which the transmitted force change its sign passing from negative to positive, and the contact between sleeve and idle gear occurs on the other teeth flank.

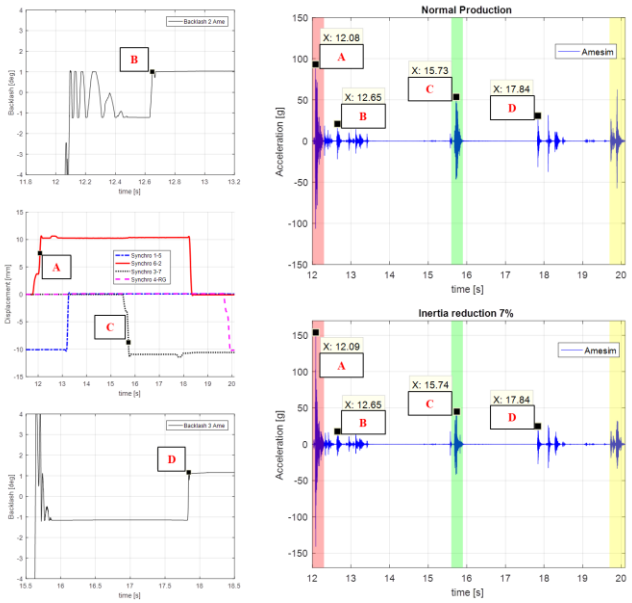

Figure 23. Upshift acceleration and inner evets of the gearbox.

During this upshift manoeuver an inertia reduction leads to positive benefits for the cross-shift noise, and for the 3rd gear engagement noise, even if a worsening in the 2nd gear engagement happens.

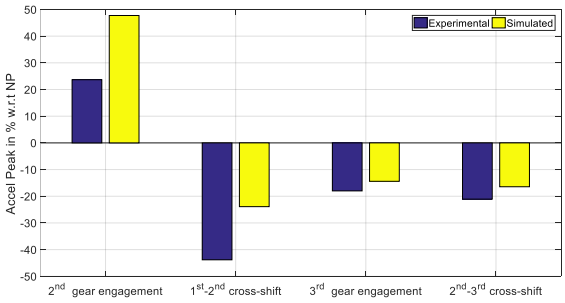

Figure 24. Comparison of experimental and simulated results.

From Figure 24 it is clear that inertia reduction has a similar effect in experimental and simulated results. The improvement over NP (normal production configuration) is more pronounced in the experimental data than in the simulation, while for the 2nd gear engagement the worsening with respect to NP is greater in the simulated results. The good match between experimental and simulated results is primarily due to the high level of detail of the physical model that is able to describe the main internal dynamics of the gearbox involved in the gearshift noise generation.

Conclusions

In this paper a novel methodology for the assessment of the gear shift noise in a Dual Clutch Transmission has been proposed and proven to be effective to compare design solutions in the transmission NVH perspective. A nonlinear lumped parameters model and a post processing tool for the evaluation of the gearbox housing acceleration starting from the bearing forces has been discussed. The peak value of the acceleration time history, used as metric for the clunking noise assessment, provided a useful instrument to compare the instantaneous and localized impact in the transmission. The most critical events producing impact in the driveline are highlighted and discussed starting from experimental data. It has been shown that during a gearshift manoeuver, the noise issues are significantly affected by the gear engagement/disengagement, clutch engagement/disengagement and load reversal that produce acceleration peaks well correlated to the subjective noise perception in the car. Moreover, the experimental analysis about the effect of inertia reduction is in deep agreement with the simulated results.

References

1. Qatu, M.S., Abdelhamid, M.K., Pang, J., Sheng, G., "Overview of automotive noise and vibration", Int. J. Vehicle Noise and Vibration, Vol. 5, Nos. 1/2, 2009, pp. 1-35, doi:10.1504/IJVNV.2009.029187.
2. Le Guen, D., Weck, T., Balihe, A., Verbeke, B., "Definition of gearshift pattern: innovative optimization procedures using system simulation", SAE Int. J. Engines, Volume 4, Issue 1, 2011, pp. 412-431, doi:10.4271/2011-01-0395.
3. Chen, M., Wang, D., Lee, H., Jiang, C. et al., "Application of CAE in Design Optimization of a Wet Dual Cutch Transmission and Driveline," SAE Int. J. Passeng. Cars - Mech. Syst. 7(3): 1128-1137, 2014, doi:10.4271/2014-01-1755.
4. Shih, S., Yruma, J., and Kittredge, P., "Drivetrain Noise and Vibration Troubleshooting," SAE Technical Paper 2001-01-2809, 2001, doi:10.4271/2001-01-2809.
5. Brancati, R., Rocca, E., Russo, R., "A gear rattle model accounting for oil squeeze between the meshing gear teeth", Proceedings of IMechE-PartD, Journal of Automobile Engineering 219 (9), 2005, pp.1075–1083.
6. Russo, R., Brancati, R., Rocca, E., "Experimental investigations about the influence of oil lubricant between teeth on the gear rattle phenomenon", Journal of Sound and Vibration, Vol. 321, Issues 3–5, 10 April 2009, pp. 647-661, ISSN 0022-460X, doi:10.1016/j.jsv.2008.10.008.
7. Miyasato, H. H., Milton, D. J., Simionatto, V. G. S., "Study of the gear rattle phenomena in automotive powertrain systems ", 21st International Congress Of Mechanical Engineering, 21-28 October 2011, Brazil.
8. Brancati, R., Rocca, E., Savino, S., "A gear rattle metric based on the wavelet multi-resolution analysis: Experimental investigation", Mechanical Systems and Signal Processing, Vol. 50–51, January 2015, pp. 161-173, ISSN 0888-3270, doi: 10.1016/j.ymssp.2014.05.018.
9. Zhang, Z., Pang, J., Li, H., Yang, X., et al., "Study Of Dual-Clutch Transmission Gear Rattle Under Low Speed Driving Condition", ICSV22, Florence (Italy) 12-16 July 2015.
10. Galvagno, E., Guercioni, G., and Vigliani, A., "Sensitivity Analysis of the Design Parameters of a Dual-Clutch Transmission Focused on NVH performance", SAE Technical Paper 2016-01-1127, 2016, doi:10.4271/2016-01-1127.
11. Galvagno, E., Tota, A., Velardocchia, M., and Vigliani, A., "Enhancing Transmission NVH Performance through Powertrain Control Integration with Active Braking System," SAE Technical Paper 2017-01-1778, 2017, https://doi.org/10.4271/2017-01-1778.
12. Walker, P. D., Zhang, N., "Investigation of synchroniser engagement in dual clutch transmission equipped powertrains", Journal of Sound and Vibration, Vol. 331, Issue 6, 2012, pp. 1398-1412, doi:10.1016/j.jsv.2011.11.005.
13. Razzacki, S. and Hottenstein, J., "Synchronizer Design and Development for Dual Clutch Transmission (DCT)," SAE Technical Paper 2007-01-0114, 2007, doi:10.4271/2007-01-0114.
14. Pacejka, H.B., "Tyre and vehicle dynamics", 2006, Butterworth, Stoneham.
15. SKF Industrie S.p.A., "SKF rolling bearings catalogue", 6000 IT, 2006.

Contact Information

enrico.galvagno@polito.it